



**HAL**  
open science

## Effect of high pressure homogenization on the structure and the interfacial and emulsifying properties of $\beta$ -lactoglobulin

Ali Ali, Isabelle Le Potier, Nicolas Huang, Véronique Rosilio, Monique Cheron, Vincent Faivre, Isabelle Turbica, Florence Agnely, Ghazlene Mekhloufi

### ► To cite this version:

Ali Ali, Isabelle Le Potier, Nicolas Huang, Véronique Rosilio, Monique Cheron, et al.. Effect of high pressure homogenization on the structure and the interfacial and emulsifying properties of  $\beta$ -lactoglobulin. *International Journal of Pharmaceutics*, 2018, 537 (1-2), pp.111-121. 10.1016/j.ijpharm.2017.12.019 . hal-04269446

**HAL Id: hal-04269446**

**<https://hal.science/hal-04269446>**

Submitted on 5 Jun 2024

**HAL** is a multi-disciplinary open access archive for the deposit and dissemination of scientific research documents, whether they are published or not. The documents may come from teaching and research institutions in France or abroad, or from public or private research centers.

L'archive ouverte pluridisciplinaire **HAL**, est destinée au dépôt et à la diffusion de documents scientifiques de niveau recherche, publiés ou non, émanant des établissements d'enseignement et de recherche français ou étrangers, des laboratoires publics ou privés.

# Effect of high pressure homogenization on the structure and the interfacial and emulsifying properties of $\beta$ -lactoglobulin

Ali Ali<sup>a</sup>, Isabelle Le Potier<sup>b</sup>, Nicolas Huang<sup>a</sup>, Véronique Rosilio<sup>a</sup>, Monique Cheron<sup>c</sup>,  
Vincent Faivre<sup>a</sup>, Isabelle Turbica<sup>d</sup>, Florence Agnely<sup>a,°</sup>, Ghozlene Mekhloufi<sup>a,°,\*</sup>

<sup>a</sup> Institut Galien Paris-Sud, CNRS, Univ. Paris-Sud, Université Paris-Saclay, 5 rue Jean-Baptiste Clément, 92296, Châtenay-Malabry Cedex, France

<sup>b</sup> Centre de Nanosciences et de Nanotechnologies, UMR CNRS 9001, Univ. Paris Sud, Université Paris Saclay, C2N – Marcoussis, 91460 Marcoussis, France.

<sup>c</sup> Pierre et Marie Curie University, Laboratoire Jean Perrin, Paris, France

<sup>d</sup> INSERM, UMR-S 996, Inflammation, Chemokines and Immunopathology, Châtenay-Malabry, France.

<sup>°</sup> Equal contribution

\*Corresponding Author

E-mail: ghozlene.mekhloufi@u-psud.fr

## Abstract

The effect of high pressure homogenization (HPH) on the structure of  $\beta$ -lactoglobulin ( $\beta$ -lg) was studied by combining spectroscopic, chromatographic, and electrophoretic methods. The consequences of the resulting structure modifications on oil/water (O/W) interfacial properties were also assessed. Moderated HPH treatment (100 MPa/4 cycles) showed no significant modification of protein structure and interfacial properties. However, a harsher HPH treatment (300 MPa/5 cycles) induced structural transformation, mainly from  $\beta$ -sheets to random coils, wide loss in lipocalin core, and protein aggregation via intermolecular disulfide bridges. HPH-modified  $\beta$ -lg displayed higher surface hydrophobicity leading to a faster adsorption rate at the interface and an earlier formation of an elastic interfacial film at  $C_{\beta\text{-lg}} = 0.1$  wt%. However, no modification of the interfacial properties was observed at  $C_{\beta\text{-lg}} = 1$  wt%. At this protein concentration, the prior denaturation of  $\beta$ -lg by HPH did not modify the droplet size of nanoemulsions prepared with these  $\beta$ -lg solutions as the aqueous phases. A slightly increased creaming rate was however observed. The effects of HPH and heat denaturations appeared qualitatively similar, but with differences in their extent.

**Keywords:**  $\beta$ -lactoglobulin; protein structure; high pressure homogenization; heat denaturation; interfacial properties; nanoemulsion.

## 1. Introduction

Nanoemulsions (NEs) are emulsions with droplet size with nanometric scale (often less than 200 nm). The relatively small droplet size confers to them a high stability to gravitational separation and a high surface-to-volume ratio (Tadros et al., 2004). NEs are very attractive systems for the efficient delivery of lipophilic functional components, such as drugs (Singh et al., 2017), vitamins (Morais Diane and Burgess, 2014; Relkin et al., 2009), and nutraceuticals

(Sun *et al.*, 2015). The preparation of NEs requires the use of high amounts of surfactants to rapidly cover and stabilize the large interfacial area created by the nanosized droplets. However, surfactants raise toxicity and irritation concerns, which may impair the use of NEs especially in long term treatments. Proteins appear to be promising emulsifying agents for food (Adjonu *et al.*, 2014; Chu *et al.*, 2007) and pharmaceutical NEs (Ali *et al.*, 2016; He *et al.*, 2011). Indeed, due to their amphiphilic nature, they adsorb rapidly at the surface of the newly formed droplets. They form an adsorbed layer at droplets surface preventing their re-coalescence and then providing physical stability to emulsion (Dickinson, 2001). Among proteins used to stabilize NEs,  $\beta$ -lactoglobulin ( $\beta$ -lg) has been recognized to have the best emulsifying properties as it allowed obtaining the smallest nanosized droplets with the best physical stability and biocompatibility (Benjamins, 2000; He *et al.*, 2011; Smulders, 2000).

$\beta$ -lg is a small globular protein belonging to the lipocalin family. It represents the major whey protein in ruminant species. The monomer of  $\beta$ -lg is composed of 162 amino acids with a molecular weight of 18 350 g.mol<sup>-1</sup>. Several genetic variants exist. The most common ones are  $\beta$ -lg A and  $\beta$ -lg B that differ only at two positions 64 and 118, which are Asp and Val for variant A and Gly and Ala for variant B (Meza-Nieto *et al.*, 2007). The secondary structure of  $\beta$ -lg is composed of eight antiparallel  $\beta$ -sheets forming a central hydrophobic cavity (called lipocalin core) and one  $\alpha$ -helix. A ninth  $\beta$ -sheet forms a part of the homodimer interface.  $\beta$ -lg contains five cysteine residues; four of them form two disulfide bridges (Cys<sup>66</sup>-Cys<sup>160</sup> and Cys<sup>106</sup>-Cys<sup>119</sup>) and the fifth one, Cys<sup>121</sup>, is free and is buried in a small hydrophobic pocket located at the outer face of the protein molecule between the lipocalin core and the  $\alpha$ -helix structure (Braunitzer *et al.*, 1973; Brownlow *et al.*, 1997; Monaco *et al.*, 1987).

High pressure (HP) treatment, also called static HP, was widely studied on proteins and more specifically on  $\beta$ -lg as a process of sterilization and microbial deactivation in the food industry (Hayashi, 1992; Knudsen *et al.*, 2004). The high pressure homogenization (HPH)

widely used in the pharmaceutical field because of its scalability as a high energy emulsification method is a radically different process that combines several mechanisms. In the HPH process, so called dynamic HP, the sample is subjected to HP and, consequently, forced to pass through a narrow valve. The flow pattern of the sample at the end of the valve depends on its design, the applied pressure value, and the sample composition and viscosity. The flow regime determines the importance of turbulence, shear, and cavitation, the main mechanisms responsible for the disruption of the oil droplets. These mechanical forces are accompanied by a short life heating phenomenon. Simultaneously, the resulting droplets can re-coalesce depending on the same forces (Cortés-Muñoz *et al.*, 2009; Flourey *et al.*, 2004; Grácia-Juliá *et al.*, 2008; Walstra, 1983). High pressure emulsification can also be performed using the high pressure microfluidization (HPM) process which has a similar principle as the HPH except that the impact force is higher (McClements, 2011). It has been reported that HPH could denature proteins (Paquin, 1999), and probably alter their emulsifying properties (Bader *et al.*, 2011; Lee *et al.*, 2009). Up to now the denaturation of  $\beta$ -lg was observed when bovine milk was HPH-treated at pressure values  $\geq 150$  MPa (Hayes *et al.*, 2005; Zamora *et al.*, 2012). The studies of the effect of HPH or HPM on proteins have mainly dealt with proteins flexibility, susceptibility to enzymatic hydrolysis, and digestibility (Blayo *et al.*, 2016; Toro-Funes *et al.*, 2014). Regarding the interfacial properties, studies were carried out on the entire whey protein and showed that this treatment improved the foaming and the emulsifying efficiencies by disaggregating the large particles of protein (Bouaouina *et al.*, 2006; Dissanayake and Vasiljevic, 2009). Other studies have shown that HPH induced whey protein aggregation when the protein was initially exempt of aggregates (Grácia-Juliá *et al.*, 2008). Whey protein is composed mainly of  $\beta$ -lg ( $\approx 50$  %) and  $\alpha$ -lactalbumin ( $\alpha$ -la  $\approx 20$  %), with minor amounts of others globular proteins (Walstra and Jenness, 1984). These proteins could be differently affected under HPH-treatment and interact in such a way that it is not possible to establish a

reliable relation between structural modifications and emulsifying efficiency. However, to the best of our knowledge, the effect of the dynamic HPH-treatment on the structure of the purified  $\beta$ -lg was only studied once, and solely on the secondary structure by Fourier transform infrared spectroscopy at a pressure value of 140 MPa. Under these conditions, no effect on the protein structure was observed (Subirade *et al.*, 1998). Other studies dealt with the reduction in  $\beta$ -lg antigenicity due to HPM-induced aggregation (Zhong *et al.*, 2012; Zhong *et al.* 2014), and there are no data on the effect of the HPH-treatment on the interfacial or emulsifying properties of  $\beta$ -lg.

Conversely, the heat-denaturation of  $\beta$ -lg has been extensively studied and its mechanism is quite well understood. It could be summarized as follows. Heat treatment disrupts the intramolecular hydrogen bonds network of the native  $\beta$ -lg. It induces the protein unfolding and the exposure of the hydrophobic core and, consequently, it increases the surface hydrophobicity. Moreover, the free thiol group (SH<sup>121</sup>) and probably the non-native free thiol group (SH<sup>119</sup>) are also exposed. Aggregates would be formed via both types of intermolecular interactions: covalent (disulfide bonds) and non-covalent (hydrophobic and electrostatic) (Croguennec *et al.*, 2003; Iametti *et al.*, 1996; Hoffmann and van Mil, 1997). The increase in the surface hydrophobicity by heat-denaturation was assumed to improve the emulsifying efficiency when emulsions were prepared by HPH (Kim *et al.*, 2005; Knudsen *et al.*, 2008). However, opposite results were obtained using high-speed mixers (Moro *et al.*, 2013).

In a previous study, we prepared oil/water (O/W) NEs stabilized by  $\beta$ -lg intended for a pharmaceutical application by using HPH (Ali *et al.*, 2016). We found that the optimum process conditions for the formulation were obtained at moderate HPH treatment (100 MPa/4 cycles). In those experimental conditions, the smallest droplets (size close to 200 nm) with a monomodal distribution were formed with the lowest energy expense. At harsher HPH conditions, 300 MPa, the droplet size increased when the number of cycles in the homogenizer

was between 3 and 5 cycles. Thus, 5 cycles and 300 MPa corresponded to the most severe conditions and potentially to the most denaturing conditions investigated. The aim of the present work was to study more thoroughly the effect of HPH in both treatment conditions (100 MPa/4 cycles and 300 MPa/5 cycles) on the secondary, tertiary and quaternary structures of the  $\beta$ -lg in phosphate buffer solution, and subsequently on its O/W interfacial and emulsifying properties. This work intends to gain a better understanding of the mechanism of the HP emulsification with globular proteins as emulsifiers. Based on the numerous works on the heat-denaturation of  $\beta$ -lg, the heat-treatment at 85 °C/30 min is sufficient to induce significant changes in its secondary, tertiary, and quaternary structures (Croguennec et al., 2004; Rada-Mendoza, 2006). Thus, this treatment was used as reference of widely denatured  $\beta$ -lg.

## **2. Material and methods**

### **2.1. Preparation of protein solutions**

$\beta$ -lg (Lot SLBC2933V, Sigma Aldrich Chemical Co., USA) solutions in 10 mM potassium phosphate buffer solution (PBS, pH 7.0) were prepared by the method previously reported (Ali et al., 2016) at the protein concentration  $C_{\beta\text{-lg}} = 1$  wt%. The protein concentration was checked by a V530 UV/vis spectrophotometer (Jasco, Japan) at 278 nm, using the specific extinction coefficient of  $9.6 \text{ dl.cm}^{-1}.\text{g}^{-1}$  (Townend et al., 1960).  $\beta$ -lg was used as received without further purification. The supplier specifications indicate that the  $\beta$ -lg product is a lyophilized powder with a purity of  $\geq 90\%$  (99.20% by PAGE for the batch used in this work). Protein standard solutions for size exclusion chromatography were prepared similarly in the ultra-purified water at the concentration  $C_{\beta\text{-lg}} = 0.1$  wt%.

### **2.2. High pressure homogenization- and heat-treatments on $\beta$ -lg solutions**

1 wt%  $\beta$ -lg solutions were passed through a HP homogenizer Stansted (Stansted Fluid Power, UK) equipped with a 10 mL processing cell and operating at 40 °C. The processing conditions

selected were 100 MPa/4 cycles and 300 MPa/5 cycles. Heat-denaturation was carried out on 3 mL of 1 wt%  $\beta$ -lg solution in a water bath maintained at 85 °C during 30 min. Then, samples were immediately cooled down in a water bath at room temperature.

### **2.3. $\beta$ -lg characterization**

#### **2.3.1. Reversed Phase - High Performance Liquid Chromatography (RP-HPLC)**

RP-HPLC analysis of  $\beta$ -lg was performed using an automated HPLC System consisting of a Waters 600 Controller pump, a Waters 717 plus autosampler, an octyl-bonded silica gel column (Discovery BIO Wide Pore C8, 25 cm  $\times$  4.6 mm, 5  $\mu$ m), a Waters 486 Tunable Absorbance detector, and Azur (DATALYS, France) as a data acquisition system.

Mobile phase was composed of solvent-1, (HPLC-grade water/acetonitrile (93/7 v/v%) with trifluoroacetic acid (0.1 v/v%)) and solvent-2 (HPLC-grade water/acetonitrile (7/93 v/v%) with trifluoroacetic acid (0.1 v/v%)). The  $\beta$ -lg solutions were diluted tenfold with PBS to reach a protein concentration  $C_{\beta\text{-lg}} = 0.1$  wt%. 25  $\mu$ L of samples were injected into the column and eluted at a flow rate of 1 mL.min<sup>-1</sup> with 70% of solvent-1 for 5 min followed by a linear gradient of 30 – 57% of solvent-2 over 35 min. Column temperature was maintained at 25 °C. The column was stabilized at initial conditions during 30 min before the next injection. Peak detection was performed at 214 nm. Standard protein solutions of  $\beta$ -lg A,  $\beta$ -lg B,  $\alpha$ -la, and BSA (Bovine Serum Albumin) (Sigma Aldrich Chemical Co., USA) at  $C_{\beta\text{-lg}} = 0.1$  wt% were analyzed similarly. For protein quantity estimations, the chromatogram peaks were deconvoluted by Gaussian distribution model using Origin software program (OriginLab Co., USA). Solutions were prepared in duplicate. For each solution, dilution steps were made in duplicate. Two injections were performed for each dilution. Results are presented as the mean ( $n = 8$ ) and standard deviation of these measurements.

#### **2.3.2. Circular Dichroism (CD) measurements**

CD spectroscopy was used to quantify modifications in secondary and tertiary structures of  $\beta$ -lg and was performed using a Jasco model J810 spectropolarimeter. An optical quartz Suprasil cell (Hellma GmbH & Co., Germany) with a path length of 0.1 cm was used at room temperature. 1 wt%  $\beta$ -lg solutions were used to assess the tertiary structure in the near-UV region (340 – 260 nm). The same solutions were diluted twenty fold in PBS to scan the secondary structure in the far-UV region (250 – 200 nm). The scanning conditions were 0.5 nm of data interval, 1 nm of bandwidth, 0.1 nm of resolution and 50 nm.min<sup>-1</sup> of scan speed, corrected by subtracting the buffer baseline spectrum. The results were expressed in mean residue ellipticity  $[\theta]$  (deg.cm<sup>2</sup>.dmol<sup>-1</sup>) (Kelly and Price, 1997).

The secondary structure estimation was carried out from the available far-UV CD spectrum by the method of Chen (Chen *et al.*, 1974) where the observed mean residue ellipticity  $[\theta]$  at a fixed wavelength is a linear combination of the mean residue ellipticity values of the  $\alpha$ -helix  $[\theta]_{\alpha}$ ,  $\beta$ -sheets  $[\theta]_{\beta}$ , and of random coils  $[\theta]_c$  at the same wavelength as follows (equation 1):

$$[\theta] = f_{\alpha}[\theta]_{\alpha} + f_{\beta}[\theta]_{\beta} + f_c[\theta]_c \quad (1)$$

where  $f_{\alpha}$ ,  $f_{\beta}$ , and  $f_c$  are the fractions of  $\alpha$ -helix,  $\beta$ -sheets, and random coils, respectively. The reference mean residue ellipticity values used  $[\theta]_{\alpha}$ ,  $[\theta]_{\beta}$ , and  $[\theta]_c$  were those reported by Greenfield and Fasman (1969) for poly(L-lysine). The values of  $f_{\alpha}$ ,  $f_{\beta}$ , and  $f_c$  were estimated by a least-squares fitting with a constraint of  $f_{\alpha} + f_{\beta} + f_c = 1$ . Experiments were carried out in triplicate at least.

### **2.3.3. Size-Exclusion Chromatography (SEC)**

SEC measurement was achieved on a HPLC gel filtration column (TSK G3000SW, 300 × 7.5 mm, column N° 3SW 321GM0249, Tosoh Biosep GmbH, Germany) with a calibration range of 10 000 – 500 000 g.mol<sup>-1</sup>. The HPLC system consisted of an isocratic

pump (Jasco PU-980 Intelligent HPLC pump, Jasco International Co., Japan), UV detector (Jasco 875 UV Intelligent UV/VIS detector, Jasco International Co., Japan), and Azur (DATAALYS, France) as a data acquisition system. The mobile phase was composed of 10 mM PBS (pH 7.0), previously filtered in a 0.2  $\mu\text{m}$  nylon membrane filter (Pall Co., USA). 25  $\mu\text{L}$  of samples were injected and eluted out with a flow rate of 0.4  $\text{mL}\cdot\text{min}^{-1}$  at room temperature. Peak detection was at 280 nm. Apparent molecular weight ( $\overline{Mw}_{\text{SEC}}$ ) was calculated using the calibration curve ( $R^2 \geq 0.90$ ) which was elaborated using six standards:  $\beta$ -amylase (200 000  $\text{g}\cdot\text{mol}^{-1}$ ), alcohol dehydrogenase (150 000  $\text{g}\cdot\text{mol}^{-1}$ ), bovine serum albumin BSA (66 000  $\text{g}\cdot\text{mol}^{-1}$ ), ovalbumin (46 000  $\text{g}\cdot\text{mol}^{-1}$ ), carbonic anhydrase (29 000  $\text{g}\cdot\text{mol}^{-1}$ ), and  $\beta$ -lg B (18 400  $\text{g}\cdot\text{mol}^{-1}$ ) (Sigma Aldrich Chemical Co., USA). The experiments were performed in duplicate.

#### **2.3.4. Sodium Dodecyl Sulfate - Polyacrylamide Gel Electrophoresis (SDS-PAGE)**

PAGE trials under denaturing non-reducing conditions (SDS-PAGE) was carried out using separating gel 12 w/v% (37.5 v/v% 1 M Tris pH 8.8; 30 v/v% acrylamide/bis-acrylamide 29:1 solution; 32.5 v/v% water with 1.5 v/v%, ammonium persulfate APS 10 w/v%, 0.5 v/v% SDS solution 20 w/v%, and 0.1 v/v% tetramethylethylenediamine TEMED) with stacking gel 4 w/v% (12.6 v/v% 1 M Tris pH 8.8; 11.5 v/v% acrylamide/bis-acrylamide 29:1 solution; 75.9 v/v% water; with 1.7 v/v% APS 10 w/v%, 0.5 v/v% SDS solution 20 w/v%, and 0.3 v/v% TEMED). Before applying to gel,  $\beta$ -lg solutions were diluted tenfold with PBS (10 mM, pH 7.0) to reach a protein concentration  $C_{\beta\text{-lg}} = 0.1 \text{ wt}\%$ . 100  $\mu\text{L}$  of the later solution were mixed with 20  $\mu\text{L}$  of glycerol solution (59 wt% glycerol; 29 wt% 1 M Tris pH 6.8; 12 wt% SDS, with 0.02 wt% bromophenol blue), vortexed and heated at 100° C for 5 min, and then centrifuged. Aliquots of 10  $\mu\text{L}$  of the sample were loaded onto the gels. Electrophoresis buffer was 0.02 M Tris pH 8.6 containing 1.45 w/v% of glycine, and 0.1 w/v% of SDS. Electrophoresis was carried out at room temperature at 130 V.

PAGE experiments under denaturing reducing conditions in the presence of 2-mercaptoethanol (SDS-PAGE, 2-ME) were performed according to the same protocol with addition of 6 wt% 2-ME to the glycerol solution.

After injection, the gels were placed in the staining solution (0.25 w/v% Coomassie Brilliant Blue R 250; 23 v/v% methanol; 7 v/v% acetic acid; 70 v/v% water) for 10 min under stirring, then destained in the same solution without the Coomassie Brilliant Blue 3 times for 10 minutes followed by further destaining overnight until the background became clear. Protein bands were detected and quantified using an imaging densitometer (ChemiDoc XRS+ system) and the corresponding Image Lab quantification software (Bio-Rad, USA). Apparent molecular weight ( $\overline{Mw}_{PAGE}$ ) of different protein fractions was calculated by using a calibration curve ( $R^2 \geq 0.95$ ) which was obtained using Roti®-Mark 10-150 protein standards (Carl Roth, Germany). Solvents used were of HPLC-grade. All other chemicals used were of analytical-grade. The experiments were performed in duplicate.

### **2.3.5. Interfacial tension and interfacial rheology measurements**

Interfacial properties were studied at the O/W interface between Miglyol 812 (Cremer Oleo GmbH & Co., Germany), a medium chain triglycerides oil commonly used in the pharmaceutical industry (Buggins *et al.*, 2007), and 1 wt% or 0.01 wt%  $\beta$ -lg aqueous solutions. Solutions at  $C_{\beta\text{-lg}} = 0.01$  wt% were prepared by hundredfold dilution in PBS (10 mM, pH 7.0) of the 1 wt% solutions immediately before the measurements. Interfacial tension and rheology measurements were carried out over 6 hours at 25°C by the drop method using a drop tensiometer (Teclis, Longessaigne, France) as previously reported (Ali *et al.*, 2016). This allowed to determine the interfacial tension ( $\gamma$ ), the interfacial pressure ( $\pi = \gamma - \gamma_0$ , where  $\gamma_0 \approx 28$  mN/m is the interfacial tension at Miglyol/PBS interface), the elastic modulus ( $E'$ ), the

viscous modulus ( $E''$ ), and the dilatational complex modulus ( $|E^*|$ ) which was calculated from  $E'$  and  $E''$  according to equation 2:

$$|E^*| = \sqrt{E'^2 + E''^2} \quad (2)$$

The experiments were performed in triplicate.

### 2.3.6. Emulsifying properties of treated $\beta$ -lg

1 wt%  $\beta$ -lg solutions were divided into four aliquots and treated differently to obtain: homogenized  $\beta$ -lg at 100 MPa for 4 cycles, homogenized  $\beta$ -lg at 300 MPa for 5 cycles, heat-denatured  $\beta$ -lg at 85° C for 30 min, and untreated  $\beta$ -lg (Figure 1). Then, five NEs were prepared by HPH as reported by Ali et al. (2016) using those different  $\beta$ -lg solutions as the aqueous phases and 5 w/w% Miglyol 812 as the oily phase. Two control NEs were obtained with HPH conditions of 100 MPa/4 cycles (NE (0-100/4)) and 300 MPa/5 cycles (NE (0-300/5)) with the untreated  $\beta$ -lg as the aqueous phase. Three NEs were processed at 100 MPa/4 cycles using the homogenized or heat-denatured  $\beta$ -lg as the aqueous phases. This allowed obtaining NE (100/4-100/4), NE (300/5-100/4), and NE (85°C-100/4) (Figure 1). Each NE was prepared in triplicate. The emulsifying efficiency of treated  $\beta$ -lg was evaluated by measuring droplet size, size distribution and polydispersity index (PDI) of NEs (Zetasizer Nano ZS90, Malvern Instruments, UK) as described previously (Ali et al., 2016) and by following the physical stability of the different systems over 30 days using an optical scanning analyzer (Turbiscan classic MA2000, Formulation SA, France).

## 3. Results and discussion

### 3.1. $\beta$ -lactoglobulin composition and effect of the different treatments

The composition of  $\beta$ -lg sample was analyzed by RP-HPLC (Figure 2A) using the following protein standards:  $\beta$ -lg A and  $\beta$ -lg B (the main components of  $\beta$ -lg),  $\alpha$ -la, and BSA (the common globular whey proteins expected to be present with  $\beta$ -lg). The chromatograms of the standards  $\beta$ -lg A and  $\beta$ -lg B display each two peaks: a main peak (relative area of  $76 \pm 2$  %

and  $89 \pm 2$  %, respectively) and a second smaller peak with lower retention time ( $24 \pm 2$  % and  $11 \pm 2$  %, respectively). The main peaks correspond to  $\beta$ -lg species ( $\beta$ -lg A and  $\beta$ -lg B), while smaller peaks with lower retention times seem to correspond to more hydrophilic species. These species could be lactosylated  $\beta$ -lg by Maillard reaction with lactose present in milk if this latter was heated at temperatures above  $37$  °C. Indeed, the resulting lactosylated  $\beta$ -lg may appear in RP-HPLC chromatograms as a peak shifted to more hydrophilic regions (Czerwenka et al., 2006; Léonil et al., 1997). The  $\alpha$ -la and BSA show separated peaks at lower retention times than  $\beta$ -lg.

The untreated  $\beta$ -lg sample displays three peaks: two main peaks in region 2 ( $44 \pm 7$  %, corresponding to  $\beta$ -lg B and lactosylated  $\beta$ -lg A) and in region 3 ( $40 \pm 7$  %, corresponding to  $\beta$ -lg A), and a small peak in region 1 ( $15 \pm 5$  %, corresponding to lactosylated  $\beta$ -lg B). The  $\beta$ -lg sample did not reveal any trace of  $\alpha$ -la and BSA even at high  $\beta$ -lg concentrations up to 1 wt% (results not shown). The presence of lactosylated species in  $\beta$ -lg samples provided by the same supplier as the one used in this work has been previously reported (Holt et al., 1998). These species were probably formed during the protein preparation by the supplier.

The effects of HPH- and heat-treatments on RP-HPLC signal of  $\beta$ -lg are shown in Figure 2B. Heat-denatured  $\beta$ -lg displays three small peaks in the same regions as the ones of untreated  $\beta$ -lg, whereas the majority of the protein ( $64 \pm 11$  %) exists as a broad peak shifted to more hydrophobic region of the chromatogram (region 4), in accordance with previous RP-HPLC studies (Kehoe et al., 2011; Petit et al., 2011). Homogenized  $\beta$ -lg at 100 MPa/4 cycles displays the same chromatogram as the untreated  $\beta$ -lg without any significant peaks in the more hydrophobic region 4. Nevertheless, the total relative area under the curve (AUC) is slightly lower than the one of untreated  $\beta$ -lg and represents  $78 \pm 7$  % of the total area of the untreated protein. At 300 MPa/5 cycles, an additional broad peak ( $4 \pm 2$  %) appears in the region 4 as observed with heat-denatured  $\beta$ -lg with a relative decrease of the total AUC of

$72 \pm 12$  % compared to the total area of the untreated  $\beta$ -lg. The reduction in the AUC in the case of HPH-treatment can be attributed to a reduction in the protein quantity induced by a reduction of the protein solubility under HPH treatment as it has been previously reported for heat-denatured  $\beta$ -lg (Croguennec *et al.*, 2014; Gough and Jenness, 1962), as samples were slightly more turbid after HPH in our study. However, the results herein show that the total AUC for heat-denatured  $\beta$ -lg was  $94 \pm 8$  % of the total area of the untreated  $\beta$ -lg. Thus, no significant correlation between heat-denaturation and  $\beta$ -lg solubility could be established here. Another explanation for the AUC decrease could be the change in the extinction coefficient of the protein as a result of the change in the environment of the aromatic residues caused by the protein denaturation (Ku wajima *et al.*, 1996; Wada *et al.*, 2006).

### **3.2. Secondary and tertiary structures**

Far-UV CD spectra of proteins characterize their secondary structure (Kelly and Price, 1997). The spectrum of untreated  $\beta$ -lg (Figure 3A) presents a large negative peak around 216 nm and a zero-crossing around 202.5 nm, which is characteristic of predominant  $\beta$ -sheet structure (Townend *et al.*, 1967). The estimation of the secondary structure using equation 1 shows that the untreated  $\beta$ -lg contains  $4 \pm 2$  %,  $52 \pm 4$  %, and  $44 \pm 3$  % of  $\alpha$ -helix,  $\beta$ -sheets, and random coils, respectively. Those values are close to the ones obtained by infrared spectroscopic and X-ray crystallographic analysis (7 – 11 %, 51 – 55 %, and 36 – 39 % of  $\alpha$ -helix,  $\beta$ -sheets, and random coils, respectively) (Dong *et al.*, 1996; Monaco *et al.*, 1987; Papiz *et al.*, 1986). The CD spectrum of the heat-denatured  $\beta$ -lg shows that the negative peak shifts to shorter wavelengths (around 204 nm) with a higher  $[\theta]$  absolute value. Secondary structure estimation shows that the protein is composed of  $20 \pm 3$  %,  $25 \pm 5$  %, and  $56 \pm 2$  % of  $\alpha$ -helix,  $\beta$ -sheets and random coils, respectively. That means that an increase in  $\alpha$ -helix and random coils contents occurred to the detriment of the  $\beta$ -sheets content during the heat-denaturation. Similar spectra were reported for heat-denatured  $\beta$ -lg under quite similar experimental conditions,

which were attributed to an increase in the random coils content to the detriment of the native structures (Knudsen et al., 2008; Prabakaran and Damodaran, 1997; Moro et al., 2011). At 100 MPa/4 cycles of homogenization, the far-UV CD spectrum displays the same trend as the one of the untreated  $\beta$ -lg with similar contents of secondary structure elements ( $5 \pm 2$  %,  $47 \pm 2$  %, and  $48 \pm 2$  % of  $\alpha$ -helix,  $\beta$ -sheets, and random coils, respectively). The secondary structure of the  $\beta$ -lg was thus maintained under this treatment. Conversely, at 300 MPa/5 cycles, the CD spectrum is largely modified and is quite similar to that of heat-denatured  $\beta$ -lg ( $17 \pm 2$  %,  $30 \pm 3$  %, and  $54 \pm 3$  % of  $\alpha$ -helix,  $\beta$ -sheets, and random coils, respectively), which means that the secondary structure of  $\beta$ -lg was altered under this treatment.

Near-UV CD spectra of  $\beta$ -lg are used as a fingerprint for its tertiary structure (Kelly and Price, 1997). The spectra of untreated and 100 MPa/4 cycles homogenized  $\beta$ -lg (Figure 3B) show two major negative peaks at 292.5 and 284 nm belonging to the tryptophan residues (Trp<sup>19,61</sup>), and fine structures between 260 and 280 nm attributed to the other aromatic residues of tyrosine (Tyr<sup>20,42,99,102</sup>) and phenylalanine (Phe<sup>82,105,136,151</sup>), and to the disulfide bonds. The high elliptical activities of these aromatic residues, especially those of Trp, mean that they are buried in a chiral environment (Woody, 1996). The spectrum of heat-denatured  $\beta$ -lg shows major alteration in all negative peaks in the near-UV region especially for that of Trp revealing that the aromatic residues became exposed to a less hydrophobic environment due to the disruption of the tertiary structure (Chang et al., 1978). The disappearance of peaks belonging to the Trp indicates that the thermal treatment used in this work widely destroyed the tertiary structure of  $\beta$ -lg. The spectrum of 300 MPa/5 cycles homogenized  $\beta$ -lg shows a large decrease in  $[\theta]$  absolute values for all negative peaks in near-UV region especially for the one of Trp residues indicating a great loss (about 53%) in the tertiary structure as interpreted by the percentage changes in  $[\theta]$  at 292.5 nm with respect to the untreated  $\beta$ -lg (Tedford et al., 1999). This high percentage indicates that this treatment damages the tertiary structure, yet to a lesser

extent compared to the heat-treatment. It should be noted that the emulsification process with high pressure homogenizer is often accompanied with a temperature increase all the more important that the pressure is high (Grácia-Juliá *et al.*, 2008). In the present work, the final temperature of NE homogenized at 300 MPa was about 60 °C. Thus,  $\beta$ -lg solution was heated at 60 °C for 4 minutes (time equivalent to 5 cycles in the homogenizer) and it was found that this treatment did modify neither the secondary nor the tertiary structures (CD results in Supplementary Material 1). This shows that the temperature rise in the product is not the predominant factor inducing  $\beta$ -lg denaturation during HPH treatment.

It is worth noting that the aggregation of  $\beta$ -lg by intermolecular disulfide bonds under thermal or HPH treatments might affect its CD spectra. Disulfide bonds contribute to the CD spectrum in far-UV by a positive peak between 220 and 240 nm (Hider *et al.*, 1988). In the near-UV CD spectrum, the disulfide bonds show a broad absorption peak between 250 and 280 nm, and the intensity and the sign of this peak is dependent on the dihedral angle of the disulfide bond (Woody, 1985). In this work, a slight decrease in  $[\theta]$  absolute values was observed between 225 and 245 nm. Generally, the ellipticity resulting from the disulfide groups is weaker than the one arising from aromatic groups (Towell and Manning, 1994). In fact, the analysis of the disulfide bonds by CD has received little attention in the literature. Thus, the aggregation of the  $\beta$ -lg was investigated in this work by electrophoretic analyses (section 3.3).

### **3.3. Quaternary structure, aggregation state**

Protein aggregation under HPH-treatment has been detected in preliminary trials by dynamic light scattering (results not shown). However, the interpretation of light scattering for samples presenting polymodal distributions, as in the case of several populations of protein aggregates, is complicated, and not fairly representative (Benita and Levy, 1993; Jamting *et al.*, 2011). Thus, the  $\beta$ -lg quaternary structure was assessed by SEC (Figure 4) and SDS-PAGE (Figure 5).

SEC chromatograms of untreated  $\beta$ -lg display three peaks: a main peak containing the major quantity of the protein ( $96 \pm 1 \%$ ) with a retention time of 16.9 min and  $\overline{Mw}_{SEC} = 25\,400 \pm 300 \text{ g.mol}^{-1}$ , and two small peaks with retention times of 15.2 min ( $63\,400 \pm 500 \text{ g.mol}^{-1}$ ) and 19.2 min ( $7\,300 \pm 2\,300 \text{ g.mol}^{-1}$ ).  $\overline{Mw}_{SEC}$  corresponds to the apparent molecular weight of a mixture of monomers and dimers in equilibrium. At neutral pH,  $\beta$ -lg exists as dimers, but this equilibrium shifts towards monomers when protein concentration decreases (Croguennec *et al.*, 2003).  $\beta$ -lg solution was also diluted hundredfold before the injection (chromatogram not shown). The retention time of the main peak was shifted to longer time (17.7 min), and consequently, to a smaller  $\overline{Mw}_{SEC}$  value ( $16\,300 \pm 100 \text{ g.mol}^{-1}$ ), which is very close to the apparent molecular weight of the  $\beta$ -lg monomer. This means that the native-like dimers present in the solution at  $C_{\beta\text{-lg}} = 1 \text{ wt}\%$  have entirely dissociated into monomers, in accordance with previous studies (Croguennec *et al.*, 2003; Knudsen *et al.*, 2004, 2008; Schokker *et al.*, 1999). On the contrary, the peak with a retention time of 15.2 min of the untreated  $\beta$ -lg at  $C_{\beta\text{-lg}} = 1 \text{ wt}\%$ , which is about 3% of the total quantity, was not significantly affected by this high dilution. This fraction can be ascribed to non-native like oligomers (dimers or trimers) as previously reported (Schokker *et al.*, 1999). The tiny peak at 19.2 min was equally ascribed to non-native like monomers produced during the protein preparation that could not be attributed to the monomers-dimers equilibrium, and therefore, eluted subsequently.

Heat-denatured  $\beta$ -lg SEC pattern shows the appearance of many populations in the region of higher  $\overline{Mw}$  to the detriment of  $\beta$ -lg monomers. The peak ascribed to monomer-dimer equilibrium seems to be composed of two overlapping peaks. Additionally, the peaks corresponding to non-native like monomers (after 19.2 min) previously observed with untreated  $\beta$ -lg became slightly broader with heat treatment. During heat-denaturation, the occurrence of a second overlapping peak with a shorter retention time with respect to untreated monomers has been observed previously in similar conditions (Croguennec *et al.*, 2003; Schokker *et al.*,

1999), and attributed to modified monomers that contains non-native intramolecular disulfide bond Cys<sup>106</sup> – Cys<sup>121</sup> instead of Cys<sup>106</sup> – Cys<sup>119</sup>, and consequently, non-native free thiol group SH<sup>119</sup> (Croguennec *et al.*, 2003, 2004).

Homogenized  $\beta$ -lg at 100 MPa/4 cycles displays an almost identical chromatogram to that of untreated  $\beta$ -lg except for the slight change in non-native like monomer peak, indicating that there was no significant change in the quaternary structure of the protein. Yet, at 300 MPa/5 cycles of homogenization,  $\beta$ -lg shows similar chromatogram changes as the heat-treated  $\beta$ -lg but to a smaller extent. Unlike heat-denatured  $\beta$ -lg, the major quantity of the  $\beta$ -lg ( $83 \pm 1$  %) has remained as monomers under these severe HPH conditions.

SDS-PAGE was carried out under non-reducing (Figure 5A) and reducing (Figure 5B) conditions to assess the contribution of disulfide bonds in the heat and the HPH-induced aggregations that were observed in SEC experiments. The concentration of sodium dodecyl sulfate (SDS) added to the sample with respect to  $\beta$ -lg concentration is assumed to be sufficient to disperse all non-covalent aggregates, while the covalent intermolecular interactions remain intact. Untreated  $\beta$ -lg displays a major band ( $\approx 95\%$ ) and another weak band with  $\overline{Mw}_{\text{PAGE}}$  of  $11\,300 \pm 1\,100$  g.mol<sup>-1</sup>, and  $37\,700 \pm 3\,600$  g.mol<sup>-1</sup>, respectively. These results are consistent with the SEC chromatogram of the untreated  $\beta$ -lg. The major band corresponds to  $\beta$ -lg monomers and this indicates that the dimers observed by SEC dissociated to monomers due to the presence of SDS. Nevertheless, the denatured small oligomers are still observed in the SDS-PAGE pattern (in dimers region) despite the presence of SDS, which means that the intermolecular interactions within these dimers are covalent. Similar SDS-PAGE patterns have been reported for untreated  $\beta$ -lg provided by the same supplier as ours (Báez *et al.*, 2013).

SDS-PAGE patterns of heat-denatured  $\beta$ -lg confirm the heat-induced aggregations and their proportions as previously observed by SEC. Similarly, HPH-treated  $\beta$ -lg using both

homogenization treatment conditions presents comparable numbers of aggregate population and similar  $\overline{Mw}_{PAGE}$  within these populations (data not shown). Thus, the aggregates observed in the SEC chromatogram of heat-denatured and HPH-treated  $\beta$ -lg were mostly formed by covalent interactions.

When SDS-PAGE was carried out under reducing conditions (Figure 5B), all heat or HPH-induced aggregates were reduced to monomers. It confirms that the HPH-induced aggregates have been formed by disulfide bonds. Heat-induced aggregation through the formation of disulfide bonds during heat-treatment of  $\beta$ -lg has been extensively reported (Iametti et al., 1996; Hoffmann et al., 1997; Schokker et al., 1999). However, a weak band resists to these reducing conditions and remains in the dimer region. The quantity of the protein in this band was identical to that of untreated  $\beta$ -lg in the non-reducing SDS-PAGE. It means that untreated  $\beta$ -lg contained a fraction of small oligomers associated by covalent intermolecular interactions other than the disulfide bonds. They are probably induced by the method of preparation used by the supplier, as previously reported (Surroca et al., 2002).

### **3.4. Influence of the treatments on the interfacial properties of the protein**

Homogenized  $\beta$ -lg at 100 MPa for 4 cycles and the untreated  $\beta$ -lg appeared to have similar secondary, tertiary, and quaternary structures. Conversely after 300 MPa/5 cycles,  $\beta$ -lg exhibited a clearly modified structure since it displayed a higher percentage of random coils, a wide loss in its hydrophobic core, and covalent aggregation by disulfide bonds. Interfacial tension and rheology experiments were performed in order to assess the effect of the structural modifications of  $\beta$ -lg induced by HPH-treatment on its interfacial properties. The experiments were carried out at the Miglyol 812/PBS interface. Figure 6A shows the variations of the interfacial tension ( $\gamma$ ) with untreated, heat- or HPH-treated  $\beta$ -lg at  $C_{\beta\text{-lg}} = 1$  wt%. With the untreated  $\beta$ -lg,  $\gamma$  decreased very quickly from 28 mN.m<sup>-1</sup> ( $\gamma_0$ ) to almost 15 mN.m<sup>-1</sup>. Then, the

decrease in  $\gamma$  became slower during the first hour of measurement, and could be attributed to molecular conformational changes of  $\beta$ -lg upon its adsorption (Wüstneck et al., 1999). Figure 6C shows  $E'$  and  $E''$  for untreated and treated  $\beta$ -lg at the O/W interface. Untreated  $\beta$ -lg displayed predominant elastic properties as  $E' > E''$  from the beginning of the experiment time.  $E'$  increased over time until reaching a maximum of about  $30 \text{ mN.m}^{-1}$  at  $t \approx 4 \text{ h}$ , and then remained stable until the end of the experiment (6 h). Simultaneously,  $E''$  decreased to a minimum of about  $1 \text{ mN.m}^{-1}$ . This behavior indicates the progressive formation of an almost purely elastic film of  $\beta$ -lg at the O/W interface. Heat- and the HPH-treated  $\beta$ -lg (300 MPa/5 cycles) displayed almost identical interfacial properties as the untreated protein, despite the wide structural modifications induced during these treatments. It might seem unexpected especially for heat-treated  $\beta$ -lg, as the protein had lost its tertiary structure and exposed its hydrophobic core. An explanation for such interfacial behavior could be given by the excess of  $\beta$ -lg molecules at the O/W interface at this high bulk protein concentration ( $C_{\beta\text{-lg}} = 1 \text{ wt\%}$ ). In fact,  $\beta$ -lg generally undergoes structural rearrangement upon adsorption to O/W interfaces in order to expose its hydrophobic residues toward the oily phase (Kim et al., 2002; Sakuno et al., 2008; Zhai et al., 2011). At high protein concentration as herein, the protein molecules are presented from the beginning as a multilayer in a compact form, and thus, the interfacial molecular rearrangements are restricted (Bouyer et al., 2011; Wüstneck et al., 1999). In this interfacial configuration, the intermolecular interactions between the adsorbed protein molecules are limited, and consequently, the structural modifications induced by heat- or HPH-treatments might not have a pronounced effect on the interfacial properties. According to the work of Wüstneck et al. (1999), the absolute values of the dilatational elasticity of the  $\beta$ -lg film at the triglycerides/water interface reach a maximum when the  $\beta$ -lg molecules are adsorbed as a monolayer for concentrations ranging between  $10^{-6}$  and  $5 \times 10^{-6} \text{ mol.L}^{-1}$ . In order to avoid immediate surface saturation, the  $\beta$ -lg solutions (untreated and treated) were diluted

hundredfold prior to the interfacial measurement with PBS to reach the monolayer concentration ( $\approx 5 \times 10^{-6} \text{ mol.L}^{-1}$ ). It should be noted that this dilution probably dissociated non-covalent dimers but it did not affect the covalent aggregates. At this lower concentration, the adsorption phase for unmodified  $\beta$ -lg (untreated or 100 MPa/4 cycles homogenized) was longer and more pronounced (Figure 6B). As seen in Figure 6D, the evolution of  $E'$  of unmodified  $\beta$ -lg displayed three different phases. In the first one,  $E'$  increased slowly, mostly due to the time needed by  $\beta$ -lg to reach the interfacial monolayer. Then  $E'$  increased quickly (in the second phase) before attaining an equilibrium state (in the third phase) when the elastic film was formed. Modified  $\beta$ -lg (by heat or by homogenization at 300 MPa/5 cycles) showed faster  $\gamma$  reduction during the adsorption phase with slightly smaller values of immediate and equilibrium  $\gamma$  compared to unmodified  $\beta$ -lg (Figure 6B), in accordance with the exposure of the hydrophobic core of the molecule under these treatments. Due to the accelerated adsorption of modified  $\beta$ -lg,  $E'$  evolution started directly by the fast increase until the equilibrium phase (Figure 6D).

The viscoelastic modulus versus interfacial pressure curves ( $|E^*| - \pi$ ) (Figures 6E and F) reflect the intermolecular interactions at the O/W interface at a given interface state regardless of the adsorption kinetic (Benjamins *et al.*, 1996). A ( $|E^*| - \pi$ ) slope value of 1 is attributed to ideal behavior indicating the absence of any intramolecular or intermolecular interaction whether within the adsorbed molecules while a slope value higher than 1 is attributed to non-ideal behavior with likely lateral intermolecular interactions (Lucassen-Reynders *et al.*, 1975). At  $C_{\beta\text{-lg}} = 1 \text{ wt\%}$ , the slope values of untreated, 100 MPa/4 cycles and 300 MPa/5 cycles homogenized, and heat-denatured  $\beta$ -lg were of 11, 12, 9, and 12, respectively. This characterizes a non-ideal behavior of the interfacial film due to the presence of intermolecular interactions. However, the curves ( $|E^*| - \pi$ ) obtained and their slope values do not allow

establishing a clear relationship between the different treatments and the film nature due to the multilayer formation.

At  $C_{\beta\text{-lg}} = 0.01$  wt%, untreated and 100 MPa/4 cycles homogenized  $\beta\text{-lg}$  showed two different phases of  $(|E^*| - \pi)$  curve. The first one ( $\pi$  from 6 to 10  $\text{mN}\cdot\text{m}^{-1}$ ) displayed an almost ideal behavior as the slope values were of 1.1 for both systems. Thus, the protein was adsorbed at the interface as separated molecules with almost zero interfacial intermolecular interactions during this step. At  $\pi \approx 10$   $\text{mN}\cdot\text{m}^{-1}$ , the interfacial monolayer of  $\beta\text{-lg}$  appears to be completely formed as the intermolecular interactions started to increase. The slope values for untreated and 100 MPa/4 cycles homogenized  $\beta\text{-lg}$  were of 5 corresponding to a non-ideal interface. For heat-denatured and 300 MPa/5 cycles homogenized  $\beta\text{-lg}$ ,  $\pi$  value corresponding to the formed interfacial monolayer ( $\approx 10$   $\text{mN}\cdot\text{m}^{-1}$ ) was obtained directly. As it was not possible to measure values of  $E'$  and  $E''$  for times lower than 10 s, the smallest value of  $\pi$  for heat-denatured and 300 MPa/5 cycles homogenized  $\beta\text{-lg}$  was  $\approx 10$   $\text{mN}\cdot\text{m}^{-1}$ . Thus, the first phase of the ideal behavior was entirely absent with these treatments. The non-ideal interfacial film was formed with slope values of 6 for both treatments with slightly smaller  $|E^*|$  values compared to the unmodified protein. This means that the interfacial intermolecular interactions of the modified  $\beta\text{-lg}$  were less important than those of the unmodified protein, probably due to the presence of aggregates. However, at  $\pi$  value of  $\approx 14$   $\text{mN}\cdot\text{m}^{-1}$ , the interfacial films of treated and untreated  $\beta\text{-lg}$  attained a similar state of intermolecular interactions ( $|E^*|$  value was of  $33.9 \pm 1.5$ ,  $33.5 \pm 0.5$ ,  $34.6 \pm 0.5$ , and  $33.9 \pm 1.0$   $\text{mN}\cdot\text{m}^{-1}$  for untreated  $\beta\text{-lg}$ , 100 MPa/4 cycles homogenized  $\beta\text{-lg}$ , 300 MPa/5 cycles homogenized  $\beta\text{-lg}$ , and heat-denatured  $\beta\text{-lg}$ , respectively).

### **3.5. Emulsifying properties of the protein**

At day 0, the reference nanoemulsion, NE (0-100/4), prepared with untreated  $\beta$ -lg had a droplet size of  $201 \pm 7$  nm with a narrow droplet size distribution ( $PDI = 0.133 \pm 0.062$ ), while the other control NE (0-300/5) prepared at 300 MPa/5 cycles had a higher droplet size ( $265 \pm 20$  nm) with a bimodal distribution ( $PDI = 0.283 \pm 0.014$ ). At day 0, the three NEs prepared at 100 MPa/4 cycles with previously treated  $\beta$ -lg solutions showed mean droplet diameters and size distributions similar to that of the reference NE (0-100/4) (Figure 7). Interestingly, the protein denaturation by homogenization or heating, when performed before the nanoemulsion preparation, had no significant effect during the emulsifying process. The higher droplet size obtained when emulsification was performed at 300 MPa/5 cycles (NE (0-300/5)) could not be attributed only to the overprocessing phenomenon as the droplet size did not remain constant but increased from 1 to 5 cycles (Ali *et al.*, 2016). The higher droplet size of the formulation NE (0-300/5) might be explained by the re-coalescence of droplets during homogenization. Indeed, the highly turbulent flow under high pressure conditions could be sufficient to provoke strong collisions between previously formed droplets and, consequently, their re-coalescence. In this case, protein denaturation might not be involved in the droplet growth mechanism. Another explanation can also be proposed. The protein denaturation during the emulsification could induce the formation of inter-droplets disulfide bridges between  $\beta$ -lg molecules adsorbed onto the surface of different droplets. These intermolecular disulfide bridges could not be formed between droplets when protein denaturation was performed before emulsification as the bridges would already be formed between free  $\beta$ -lg molecules in solution. This would explain why no size increase was observed when the denaturing treatment (300 MPa/5 cycles) was applied before the nano-emulsification process at 100 MPa/4 cycles (NE (300 /5-100 /4) compared to NE (0-300/5)).

Macroscopically, all NEs appeared stable for 30 days except the NE (0-300/5) which showed a visible creaming between days 15 and 30. The droplet size remained almost unchanged for all

NEs during 30 days (Figure 7). The ratio of protein/oily phase was found to be sufficient to form an interfacial film that insured the stability of droplets against the irreversible growth phenomena such as coalescence and Ostwald ripening. These results could be explained by the similar nature of the interfacial film of  $\beta$ -lg once the NEs are obtained. Beside the difference in the adsorption kinetic of protein to the O/W interface and the resulting difference in the interfacial properties during the first hours as shown in Section 3.4, the interfacial film is likely to have the same nature at  $t \approx 4$  h for untreated, homogenized, and heat-denatured  $\beta$ -lg solutions. Physical stability of the NEs was also evaluated using the optical scanning analyzer. The backscattered intensity profiles as a function of the height of the samples are given in Supplementary Materials 2. The presence of a creaming destabilization phenomenon was detected in all NEs. The extent of creaming in NE (0-300/5) was more important and it affected the entire height of the sample. The main reason of the stability reduction in this system could be attributed to the higher droplet size ( $\sim 265$  nm) in accordance with Stokes' law. The extent of the creaming present in NE (300/5-100/4) and NE (85° C-100/4) seemed to be intermediate between the ones obtained with NE (0-100/4) or NE (100/4-100/4) (the lowest) and NE (0-300/5) (the highest).

Therefore, all treated (heated or homogenized) and untreated  $\beta$ -lg solutions showed a similar emulsifying efficiency with regards to droplet size when the emulsification process was conducted under mild conditions (100 MPa/4 cycles). However, the NEs were slightly less stable over time against creaming when  $\beta$ -lg solutions were homogenized at 300 MPa/5 cycles, or heated at 85°C before emulsification.

#### **4. Conclusion**

HPH at moderated treatment conditions (100 MPa/4 cycles) had no significant effect on  $\beta$ -lg structure or on its interfacial properties. However, following severe HPH treatment

(300 MPa/5 cycles),  $\beta$ -lg displayed an important loss in its secondary and tertiary structures, together with covalent aggregations. Structural modifications of  $\beta$ -lg caused by severe HPH treatment appeared to be comparable to those that occurred during its heat denaturation, with less extent. The exposure of the hydrophobic core of  $\beta$ -lg by the HPH or heat treatment improved the adsorption kinetic of  $\beta$ -lg at O/W interface and accelerated the formation of an elastic interfacial film at low protein concentration ( $C_{\beta\text{-lg}} = 0.01\%$ ). However, this was not the case at higher concentration ( $C_{\beta\text{-lg}} = 1\%$ ), as no difference was observed between untreated, HPH- and heat-treated  $\beta$ -lg. At this concentration, no improvement in the emulsifying efficiency of  $\beta$ -lg was achieved by protein denaturation either by HPH or by heat under the selected conditions. On the contrary, prior protein denaturation seemed to slightly increase the creaming phenomenon observed in NEs. These results contribute to improve the understanding of the emulsifying mechanism of globular protein when using high energy methods. They will be useful to design pharmaceutical NEs stabilized by globular proteins.

### **Acknowledgments**

Ali ALI acknowledges the Ministry of Higher Education of the Syrian Arab Republic for his PhD grant.

### **References**

- Adjonu, R., Doran, G., Torley, P., Agboola, S. 2014. Whey protein peptides as components of nanoemulsions: A review of emulsifying and biological functionalities. *J. Food Eng.*, 122, 15-27
- Ali, A., Mekhloufi, G., Huang, N., Agnely, F. 2016.  $\beta$ -lactoglobulin stabilized nanoemulsions - Formulation and process factors affecting droplet size and nanoemulsion stability. *Int. J. Pharm.*, 500, 291-304.

- Bader, S., Bez, J., Eisner, P. 2011. Can protein functionalities be enhanced by high-pressure homogenization ? - A study on functional properties of Lupin proteins. *Procedia Food Sci.*, 1, 1359-1366.
- Báez, G.D., Busti, P.A., Verdini, R., Delorenzi, N.J. 2013. Glycation of heat-treated  $\beta$ -lactoglobulin: Effects on foaming properties. *Food Res. Int.*, 54, 902-909.
- Benita, S., Levy, M.Y. 1993. Submicron emulsions as colloidal drug carriers for intravenous administration: Comprehensive physicochemical characterization. *J. Pharm. Sci.*, 82, 1069-1079.
- Benjamins, J., Cagna, A., Lucassen-Reynders E.H. 1996. Viscoelastic properties of triacylglycerol/water interfaces covered by proteins. *Colloids Surf., A*, 114, 245-254
- Benjamins, J. 2000. Static and dynamic properties of proteins adsorbed at liquid interfaces. Ph.D. Thesis. University of Wageningen.
- Blayo, C., Vidcoq, O., Lazenec, F., Dumay, E. 2016. Effects of high pressure processing (hydrostatic high pressure and ultra-high pressure homogenization) on whey protein native state and susceptibility to tryptic hydrolysis at atmospheric pressure. *Food Res. Int.*, 79, 40-53.
- Bouaouina, H., Desrumaux, A., Loisel, C., Legrand, J. 2006. Functionnal properties of whey proteins as affected by dynamic high-pressure treatment. *Int. Dairy J.*, 16, 275-184.
- Bouyer, E., Mekhloufi, G., Le Potier, I., du Fou de Kerdaniel, T., Grossiord, J.-L., Rosilio, V., Agnely, F. 2011. Stabilization mechanism of oil-in-water emulsions by  $\beta$ -lactoglobulin and gum arabic. *J. Colloid Interface Sci.*, 354, 467-477.
- Braunitzer, G., Chen, R., Schrank, B., Stangl, A. 1973. The sequence of  $\beta$ -lactoglobulin. *Hoppe Seylers Z Physiol Chem.*, 354, 867-878.

- Brownlow, S., Cabral, J.H.M., Cooper, R., Flower, D.R., Yewdall, S.J., Polikarpov, I. 1997. Bovine  $\beta$ -lactoglobulin at 1.8 Å resolution - Still an enigmatic lipocalin. *Structure*, 5, 481-95.
- Buggins, T.R., Dickinson, P.A., Taylor, G. 2007. The effects of pharmaceutical excipients on drug disposition. *Adv. Drug Deliv. Rev.*, 59, 1482-1503.
- Chang, C.T., Wu, C.S.C., Yang, J.T. 1978. Circular dichroic analysis of protein conformation: Inclusion of the  $\beta$ -turns. *Anal. Biochem.*, 91, 13-31.
- Chen, Y-H., Yang, J.T., Chau K.H. 1974. Determination of the helix and  $\beta$  form of proteins in aqueous solution by circular dichroism. *Biochemistry*, 13, 3350-3359.
- Chu, B.S., Ichikawa, S., Kanafusa, S., Nakajima, M. 2007. Preparation and characterization of  $\beta$ -carotene nanodispersions prepared by solvent displacement technique. *J. Agric. Food Chem.*, 55, 6754-6760.
- Cortés-Muñoz, M., Chevalier-Lucia, D., Dumay, E. 2009. Characteristics of submicron emulsions prepared by ultra-high pressure homogenization: Effect of chilled or frozen storage. *Food Hydrocolloids*, 23, 640-654.
- Croguennec, T., Bouhallab, S., Mollé, D., Kennedy, B.T.O., Mehra, R. 2003. Stable monomeric intermediate with exposed Cys-119 is formed during heat denaturation of  $\beta$ -lactoglobulin. *Biochem. Biophys. Res. Commun.*, 301, 465-471.
- Croguennec, T., O'Kennedy, B.T., Mehra, R. 2004. Heat-induced denaturation/aggregation of  $\beta$ -lactoglobulin A and B: Kinetics of the first intermediates formed. *Int. Dairy J.*, 14, 399-409.
- Croguennec, T., Leng, N., Hamon, P., Rousseau, F., Jeantet, R., Bouhallab S. 2014. Caseinomacropptide modifies the heat-induced denaturation aggregation process of  $\beta$ -lactoglobulin. *Int. Dairy J.*, 36, 55-64.

- Czerwenka, C., Maier, I., Pittner, F., Lindner, W. 2006. Investigation of the lactosylation of whey proteins by liquid chromatography-mass spectrometry. *J. Agric. Food Chem.*, 54, 8874-8882.
- Dickinson, E. 2001. Milk protein interfacial layers and the relationship to emulsion stability and rheology. *Colloids Surf B Biointerfaces*, 20, 197 – 210
- Dissanayake, M., Vasiljevic, T. 2009. Functional properties of whey proteins affected by heat treatment and hydrodynamic high-pressure shearing. *J. Dairy Sci.*, 92, 1387-1397.
- Dong, A., Matsuura, J., Allison, S. D., Chrisman, E., Manning, M.C., Carpenter, J.F. 1996. Infrared and circular dichroism spectroscopic characterization of structural differences between  $\beta$ -lactoglobulin A and B. *Biochemistry*, 35, 1450-1457.
- Floury, J., Bellettre, J., Legrand J., Desrumaux, A. 2004. Analysis of a new type of high-pressure homogeniser. A study of the flow pattern. *Chem. Eng. Sci.*, 59, 843-853.
- Gough, P., Jenness, R. 1962. Heat denaturation of  $\beta$ -lactoglobulins A and B. *J. Dairy Sci.*, 45, 1033-1039.
- Gracia-Juliá, A., René, M., Cortés-Muñoz, M., Picart, L., López-Pedemonte, T., Chevalier, D., Dumay, E. 2008. Effect of dynamic high pressure on whey protein aggregation: A comparison with the effect of continuous short-time thermal treatments. *Food Hydrocolloids*, 22, 1014-1032.
- Greenfield, N., Fasman, G. D. 1969. Computed circular dichroism spectra for the evaluation of protein conformation. *Biochemistry*, 8, 4108-4116.
- Hayashi, R. 1992. Utilization of pressure in addition to temperature in food science and technology, in: Balny, C.; Hayashi, R.; Heremans, K.; Masson, P. (Eds.), *High pressure and biotechnology*, Colloque INSERM/John Libbey Eurotext Ltd., 224, pp. 185-193.
- Hayes, M.G., Fox, P.F., Kelly, A.L. 2005. Potential applications of high pressure homogenisation in processing of liquid milk. *J. Dairy. Res.*, 72, 25-33.

- He, W., Tan, Y., Tian, Z., Chen L., Hu, F., Wu, W. 2011. Food protein-stabilized nanoemulsions as potential delivery systems for poorly water-soluble drugs: Preparation, in vitro characterization, and pharmacokinetics in rats. *Int. J. Nanomed.*, 6, 521-533.
- Hider, R.C., Drake, A.F., Tamiya, N. 1988. An analysis of the 225-230-nm CD band of Elapid toxins. *Biopolymers*, 27, 113-122.
- Hoffmann M.A.M., van Mil, P.J.J.M. 1997. Heat-induced aggregation of  $\beta$ -lactoglobulin: Role of the free thiol group and disulfide bonds. *J. Agric. Food Chem.*, 45, 2942-2948.
- Holt, C., Waninge, R., Sellers, P., Paulsson, M., Bauer R., Øgøndal, L., Roefs, S.P.F.M., van Mill, P., de Kruif, C.G., Léonil, J., Fauquant, J., Maubois, J.L. 1998. Comparison of the effect of heating on the thermal denaturation of nine different  $\beta$ -lactoglobulin preparations of genetic variants A, B or A/B, as measured by microcalorimetry. *Int. Dairy J.*, 8, 99-104.
- Iametti, S., De Gregori, B., Vecchio, G., Bonomi, F. 1996. Modifications occur at different structural levels during the heat denaturation of  $\beta$ -lactoglobulin. *Eur. J. Biochem.*, 237, 106-112.
- Jamting, Å.K., Cullen, J., Coleman, V.A., Lawn, M., Herrmann J., Miles, J., Ford, M.J. 2011. Systematic study of bimodal suspensions of latex nanoparticles using dynamic light scattering. *Adv. Powder Technol.*, 22, 290-293.
- Kehoe, J.J., Wang, L., Morris, E.R., Brodkorb, A. 2011. Formation of nonnative  $\beta$ -lactoglobulin during heat-induced denaturation. *Food Biophys.*, 6, 487-496.
- Kelly, S.M., Price N.C. 1997. The application of circular dichroism to studies of protein folding and unfolding. *Biochim. Biophys. Acta.*, 1338, 161-185.
- Kim, D.A., Cornec, M., Narsimhan, G. 2005. Effect of thermal treatment on interfacial properties of  $\beta$ -lactoglobulin. *J. Colloid Interface Sci.*, 285, 100-109.

- Kim, H.J., Decker, E.A., McClements, D.J. 2002. Role of postadsorption conformation changes of  $\beta$ -lactoglobulin on its ability to stabilize oil droplets against flocculation during heating at neutral pH. *Langmuir*, 18, 7577-7583.
- Knudsen, J.C., Lund, M., Bauer, R., Qvist, K.B. 2004. Interfacial and molecular properties of high-pressure-treated  $\beta$ -lactoglobulin B. *Langmuir*, 20, 2409-2415.
- Knudsen, J.C., Øgdenal, L.H., Skibsted, L.H. 2008. Droplet surface properties and rheology of concentrated oil in water emulsions stabilized by heat-modified  $\beta$ -lactoglobulin B. *Langmuir*, 24, 2603-2610.
- Kuwajima, K., Yamaya, H., Sugai, S. 1996. The burst-phase intermediate in the refolding of  $\beta$ -lactoglobulin studied by stopped-flow circular dichroism and absorption spectroscopy. *J. Mol. Biol.*, 264, 806-822.
- Lee, S.H., Lefèvre, T., Subirade, M., Paquin, P. 2009. Effects of ultra-high pressure homogenization on the properties and structure of interfacial protein layer in whey protein-stabilized emulsion. *Food Chem.*, 113, 191-195.
- Léonil, J., Mollé, D., Fauquant, J., Maubois, J.L., Pearce, R.J., Bouhallab, S. 1997. Characterization by ionization mass spectrometry of lactosyl  $\beta$ -lactoglobulin conjugates formed during heat treatment of milk and whey and identification of one lactose-binding site. *J. Dairy Sc.*, 80, 2270-2281.
- Lucassen-Reynders, E.H., Lucassen, J., Garrett, P.R., Hollway, F. 1975. Dynamic surface measurements as a tool to obtain equation-of-state data for soluble monolayers. *Adv. Chem. Phys.*, 144, 272-285.
- McClements, D.J. 2011. Edible nanoemulsions: Fabrication, properties, and functional performance. *Soft Matter*, 7, 2297-2316.

- Meza-Nieto, M.A., Vallejo-Cordoba, B., Gonzalez-Cordova A.F. 2007. Effect of  $\beta$ -lactoglobulin A and B whey protein variants on the rennet-induced gelation of skim milk gels in a model reconstituted skim milk system. *J. Dairy Sci.*, 90, 582-593
- Monaco, H.L., Zanotti, G., Spadon, P., Bolognesi, M., Sawyer, L., Eliopoulos, E.E. 1987. Crystal structure of the trigonal form of bovine  $\beta$ -lactoglobulin and of its complex with retinol at 2.5 Å resolution. *J. Mol. Biol.*, 197, 695-706.
- Morais Diane, J.M., Burgess, J. 2014. Vitamin E nanoemulsions characterization and analysis. *Int. J. Pharm.*, 465, 455-463.
- Moro, A., Báez, G.D., Busti, P.A., Ballerini, G.A., Delorenzi, N.J. 2011. Effects of heat-treated  $\beta$ -lactoglobulin and its aggregates on foaming properties. *Food Hydrocolloids*, 25, 1009-1015.
- Moro, A., Báez, G.D., Ballerini, G.A., Busti, P.A., Delorenzi N.J. 2013. Emulsifying and foaming properties of  $\beta$ -lactoglobulin modified by heat treatment. *Food Res. Int.*, 51, 1-7.
- Papiz, M.Z., Sawyer, L., Eliopoulos, E.E., North, A.C.T., Findlay, J.B.C., Sivaprasadarao, R., Jones, T.A., Newcomer M.E., Kraulis, P.J. 1986. The structure of  $\beta$ -lactoglobulin and its similarity to plasma retinol-binding protein. *Nature*, 324, 383-385.
- Paquin, P. 1999. Technological properties of high pressure homogenizers: The effect of fat globules, milk proteins, and polysaccharides. *Int. Dairy J.*, 9, 329-335.
- Petit, J., Herbig, A.L., Moreau, A., Delaplace, G. 2011. Influence of calcium on  $\beta$ -lactoglobulin denaturation kinetics: Implications in unfolding and aggregation mechanisms. *J. Dairy Sci.*, 94, 5794-5810.
- Prabakaran, S., Damodaran, S. 1997. Thermal unfolding of  $\beta$ -lactoglobulin: Characterization of initial unfolding events responsible for heat-induced aggregation. *J. Agric. Food Chem.*, 45, 4303-4308

- Qian, C., Decker, E.A., Xiao, H., McClements, D.J. 2012. Physical and chemical stability of  $\beta$ -carotene-enriched nanoemulsions: Influence of pH, ionic strength, temperature, and emulsifier type. *Food Chem.*, 132, 1221-1229
- Rada-Mendoza, M., Villamiel, M., Molina, E., Olano, A. 2006. Effects of heat treatment and high pressure on the subsequent lactosylation of  $\beta$ -lactoglobulin. *Food Chem.*, 99, 651-655
- Relkin, P., Jung, J.M., Ollivon, M. 2009. Factors affecting vitamin degradation in oil-in-water nanoemulsions. *J. Therm. Anal. Calorim.*, 98(1), 13-18
- Sakuno, M.M., Matsumoto, S., Kawai, S., Taihei, K., Matsumura, Y. 2008. Adsorption and structural change of  $\beta$ -lactoglobulin at the diacylglycerol-water interface. *Langmuir*, 24, 11483-11488.
- Sawyer, W.H. 1968. Heat denaturation of bovine  $\beta$ -lactoglobulin and relevance of disulfide aggregation, *J. Dairy Sci.*, 51, 323-329.
- Schokker, E.P., Singh, H., Pinder, D.N., Norris, G.E., Creamer, L.K. 1999. Characterization of intermediates formed during heat-induced aggregation of  $\beta$ -lactoglobulin AB at neutral pH. *Int. Dairy J.*, 9, 791-800.
- Singh, Y., Gopal Meher, J., Raval, K., Ali Khan, F., Chaurasia, M., Jain, N.K., Chourasia, M.K. 2017. Nanoemulsion: Concepts, development and applications in drug delivery. *J. Control. Release*, 252, 28-49
- Smulders, P.E.A. 2000. Formation and stability of emulsions made with proteins and peptides. Ph.D. Thesis, University of Wageningen.
- Subirade, M., Loupil, F., Allain, A.F., Paquin, P. 1998. Effect of dynamic high pressure on the secondary structure of  $\beta$ -lactoglobulin and on its conformational properties as determined by Fourier Transform Infrared Spectroscopy. *Int. Dairy J.*, 8, 135-140.

- Sun, Y., Xia, Z., Zheng, J., Qiu, P., Zhang, L., McClements, D.J., Xiao, H. 2015. Nanoemulsion-based delivery systems for nutraceuticals: Influence of carrier oil type on bioavailability of pterostilbene. *J. Func. Foods*, 13, 61-70
- Surroca, Y., Haverkamp, J., Heck, A.J.R. 2002. Towards the understanding of molecular mechanisms in the early stages of heat-induced aggregation of  $\beta$ -lactoglobulin AB. *J. Chromatogr. A*, 970, 275-285.
- Tadros, T., Izquierdo, P., Esquena, J., Solans, C. 2004. Formation and stability of nano-emulsions. *Adv. Colloid Interface Sci.*, 108 –109, 303–318.
- Tedford, L-A., Kelly, S.M., Price, N.C., Schaschke C.J. 1999. Interactive effects of pressure, temperature and time on the molecular structure of  $\beta$ -lactoglobulin. *J. Food Sci.*, 64, 396-399.
- Toro-Funes, N., Bosch-Fusté, J., Veciana-Nogués, M.T., Vidal-Carou, M.C. 2014. Changes of isoflavones and protein quality in soymilk pasteurised by ultra-high-pressure homogenization throughout storage. *Food Chem.*, 162, 47-53.
- Towell III, J.F., Manning, M.C. 1994. Analysis of protein structure by circular dichroism spectroscopy, in: Purdie N.; Brittain, H.G. (Eds.), *Analytical applications of circular dichroism*. Elsevier Science B.V., Amsterdam, The Netherlands. 14, pp. 175-205.
- Townend, R., Winterbottom, R.J., Timasheff, S.N. 1960. Molecular interactions in  $\beta$ -lactoglobulin. II. Ultracentrifugal and electrophoretic studies of the association of  $\beta$ -lactoglobulin below its isoelectric point. *J. Am. Chem. Soc.*, 82 (12), 3161-3168.
- Townend, R., Kumosinski, T.F., Timasheff, S.N. 1967. The circulation dichroism of variants of  $\beta$ -lactoglobulin. *J Biol Chem.*, 19, 4538–4545.
- Wada, R., Fujita, Y., Kitabatake, N. 2006. Effects of heating at neutral and acid pH on the structure of  $\beta$ -lactoglobulin A revealed by differential scanning calorimetry and circular dichroism spectroscopy. *Biochim. Biophys. Acta*, 1760, 841-847.

- Walstra, P. 1983. Formation of emulsions, in: Becher, P. (Eds.), Encyclopedia of emulsion technology: Basic theory, Marcel Dekker. 1, pp. 58-126.
- Walstra, P., Jenness, R. 1984. Dairy chemistry and physics. John Wiley and Sons, New York.
- Woody, R.W. 1985. Circular dichroism of peptides, in: Udenfried, S.; Meienhofer, J.; Hruby, V.J. (Eds.), The peptides. Academic Press, San Diego. 7, pp.15-113.
- Woody, R.W. 1996. Theory of circular dichroism of proteins, in: Fasman, G.D. (Eds.), Circular dichroism and the Conformational Analysis of Biomolecules. Plenum, New York, pp. 25-67.
- Wüstneck, R., Moser, B., Muschiolik, G. 1999. Interfacial dilational behaviour of adsorbed  $\beta$ -lactoglobulin layers at the different fluid interfaces. Colloids Surf., B, 15, 263-273.
- Zamora, A., Ferragut, V., Guamis, B., Trujillo, A.J. 2012. Changes in the surface protein of the fat globules during ultra-high pressure homogenization and conventional treatments of milk. Food Hydrocolloids, 29, 135-143.
- Zhai, J., Wooster, T.J., Hoffmann, S.V., Lee, T.H., Augustin, M.A., Aguilar, M.I. 2011. Structural rearrangement of  $\beta$ -lactoglobulin at different oil-water interfaces and its effect on emulsion stability. Langmuir, 27, 9227-9236.
- Zhong, J.Z., Liu, W., Liu, C.M., Wang, Q.H., Li, T., Tu, Z.C., Luo, S.J., Cai, X.F., Xu, Y.J. 2012. Aggregation and conformational changes of bovine  $\beta$ -lactoglobulin subjected to dynamic high-pressure microfluidization in relation to antigenicity. J. Dairy Sci., 95, 4237-4245.
- Zhong, J., Tu, Y., Liu, W., Xu, Y., Liu, C., Dun, R. 2014. Antigenicity and conformational changes of  $\beta$ -lactoglobulin by dynamic high pressure microfluidization combining with glycation treatment. J. Dairy Sci., 97, 4695-4702.

## Figure captions

**Figure 1:** Conditions for the different treatments of 1 wt%  $\beta$ -lg solutions and for nanoemulsion preparation.

**Figure 2:** RP-HPLC chromatograms of  $\beta$ -lg in 10 mM PBS (pH 7.0). (A): untreated  $\beta$ -lg (solid black line),  $\beta$ -lg A (dotted black line),  $\beta$ -lg B (dashed black line),  $\alpha$ -la (solid grey line), and BSA (dashed grey line). (B): untreated  $\beta$ -lg (solid black line),  $\beta$ -lg homogenized at 100 MPa for 4 cycles (dashed black line),  $\beta$ -lg homogenized at 300 MPa for 5 cycles (dotted black line), and heat-denatured  $\beta$ -lg at 85 °C for 30 min (solid grey line).

**Figure 3:** (A) Near-UV and (B) far-UV CD spectra of  $\beta$ -lactoglobulin in 10 mM PBS (pH 7.0) for: untreated  $\beta$ -lg (solid black line),  $\beta$ -lg homogenized at 100 MPa for 4 cycles (dashed black line),  $\beta$ -lg homogenized at 300 MPa for 5 cycles (dotted black line), and heat-denatured  $\beta$ -lg at 85 °C for 30 min (solid grey line).

**Figure 4:** SEC chromatograms of  $\beta$ -lg in 10 mM PBS (pH 7.0) for: untreated  $\beta$ -lg (solid black line),  $\beta$ -lg homogenized at 100 MPa for 4 cycles (dashed black line),  $\beta$ -lg homogenized at 300 MPa for 5 cycles (dotted black line), and heat-denatured  $\beta$ -lg at 85 °C for 30 min (solid grey line).

**Figure 5:** SDS-PAGE patterns under (A) non-reducing and (B) reducing conditions of  $\beta$ -lg in 10 mM PBS (pH 7.0) for: untreated  $\beta$ -lg (lane 1),  $\beta$ -lg homogenized at 100 MPa for 4 cycles (lane 2),  $\beta$ -lg homogenized at 300 MPa for 5 cycles (lane 3), and heat-denatured  $\beta$ -lg at 85 °C for 30 min (lane 4).

**Figure 6:** Evolution of the interfacial tension (A, B) versus time, elastic (closed symbols) and viscous modulus (open symbols) (C, D) versus time, and the complex modulus (E, F) versus the interfacial pressure between Miglyol 812 and  $\beta$ -lg solution at concentration of 1 wt% (A, C, E), or 0.01 wt% (B, D, F) for: untreated  $\beta$ -lg ( $\blacklozenge$ ),  $\beta$ -lg homogenized at

100 MPa/4 cycles (▲),  $\beta$ -lg homogenized at 300 MPa/5 cycles (■), and heat-denatured  $\beta$ -lg at 85 °C for 30 min (●).

**Figure 7:** Variation of the mean droplet diameter as a function of time for: NE (0-100/4): NE prepared at 100 MPa/4 cycles with untreated  $\beta$ -lg solution (◆); NE (0-300/5): NE prepared at 300 MPa/5 cycles with untreated  $\beta$ -lg solution (◆); NE (100/4-100/4): NE prepared at 100 MPa/4 cycles with 100 MPa/4 cycles homogenized  $\beta$ -lg solution (◆); NE (300/5-100/4): NE prepared at 100 MPa/4 cycles with 300 MPa/5 cycles homogenized  $\beta$ -lg solution (◆); and NE (85° C-100/4): NE prepared at 100 MPa/4 cycles with 85° C/30 min heat-treated  $\beta$ -lg solution (◆). Results are expressed as mean  $\pm$  standard deviation.

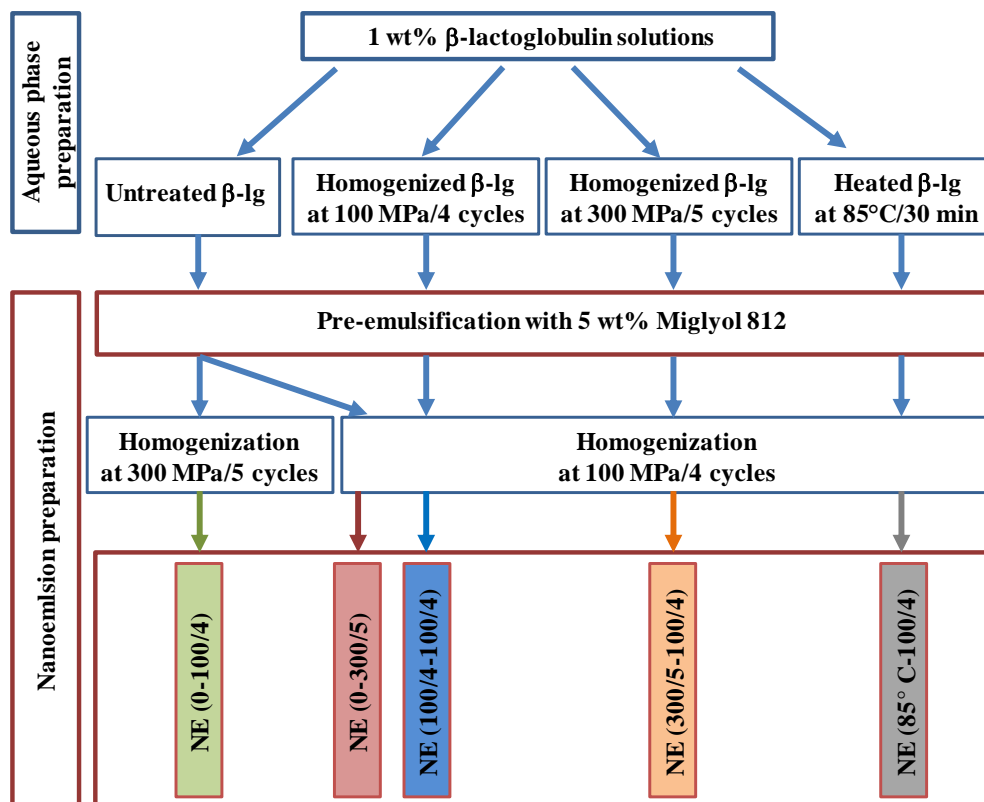


Figure 1.

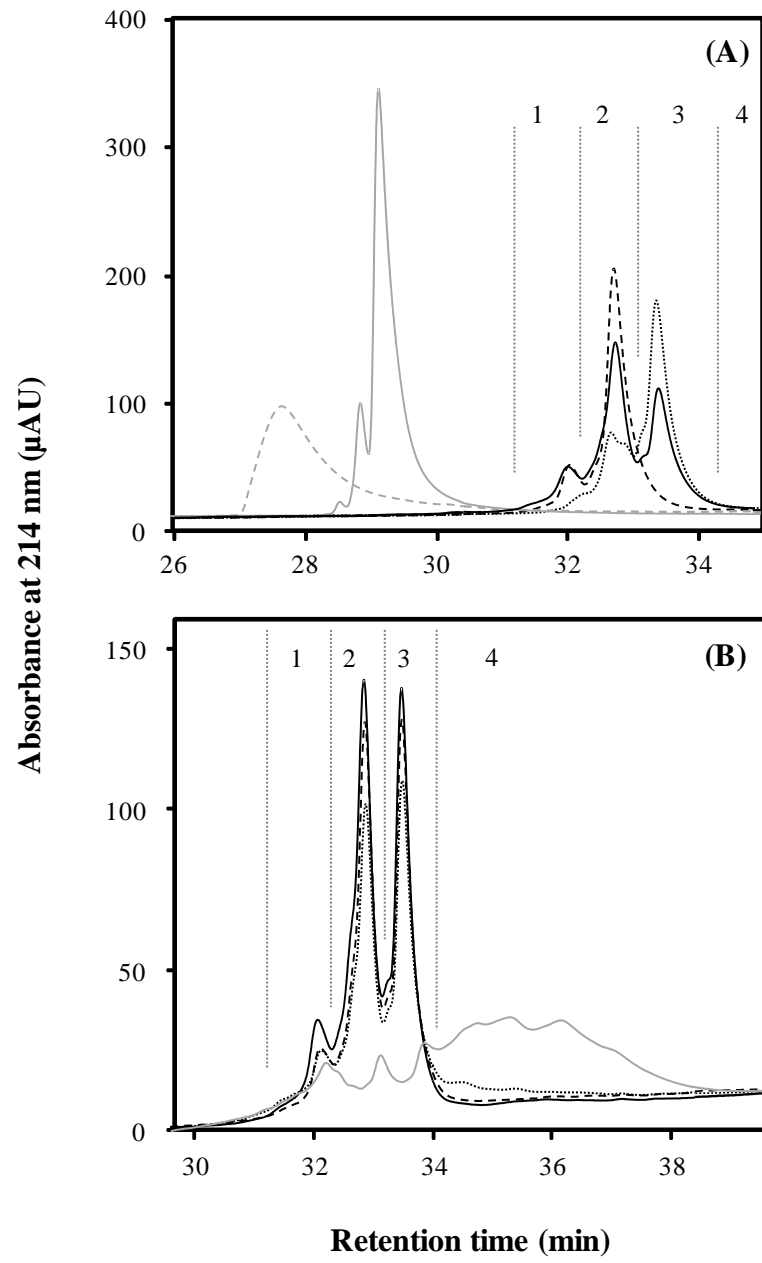


Figure 2.

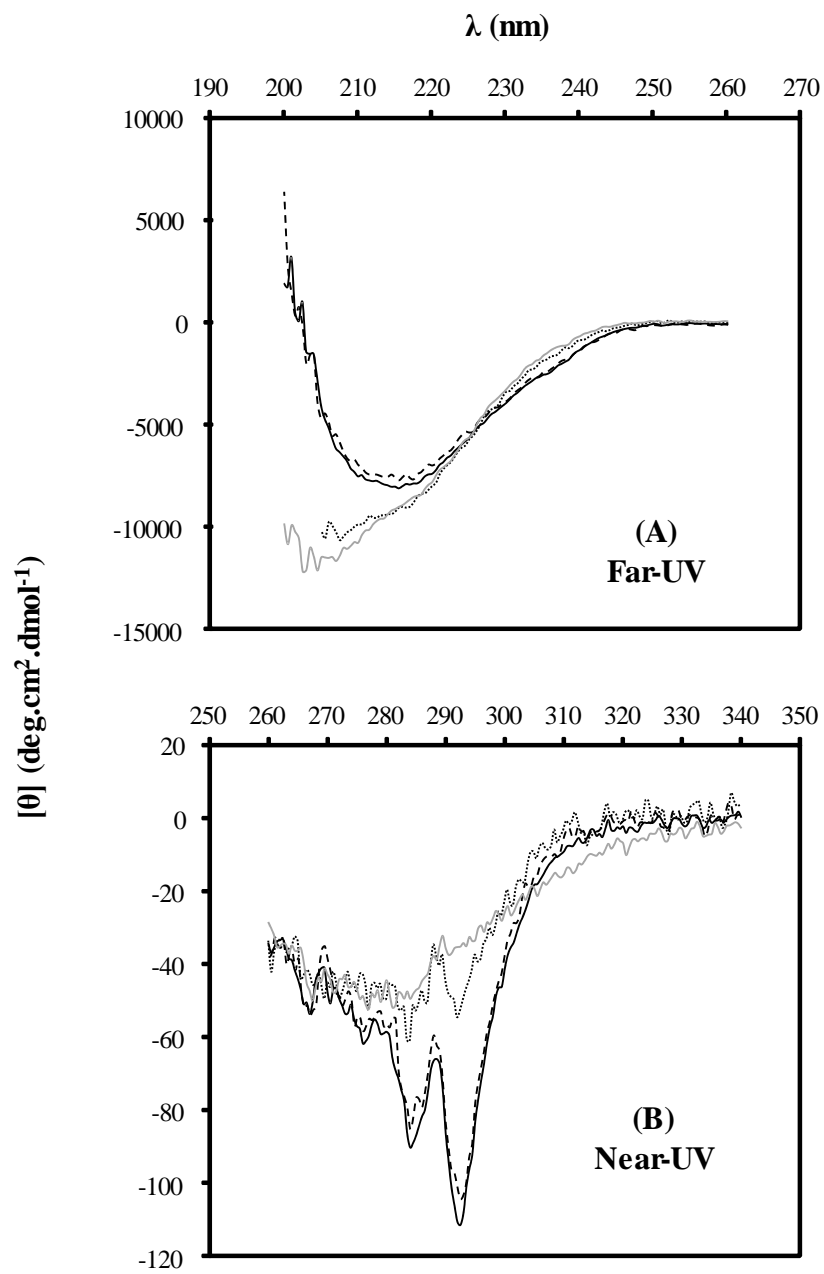
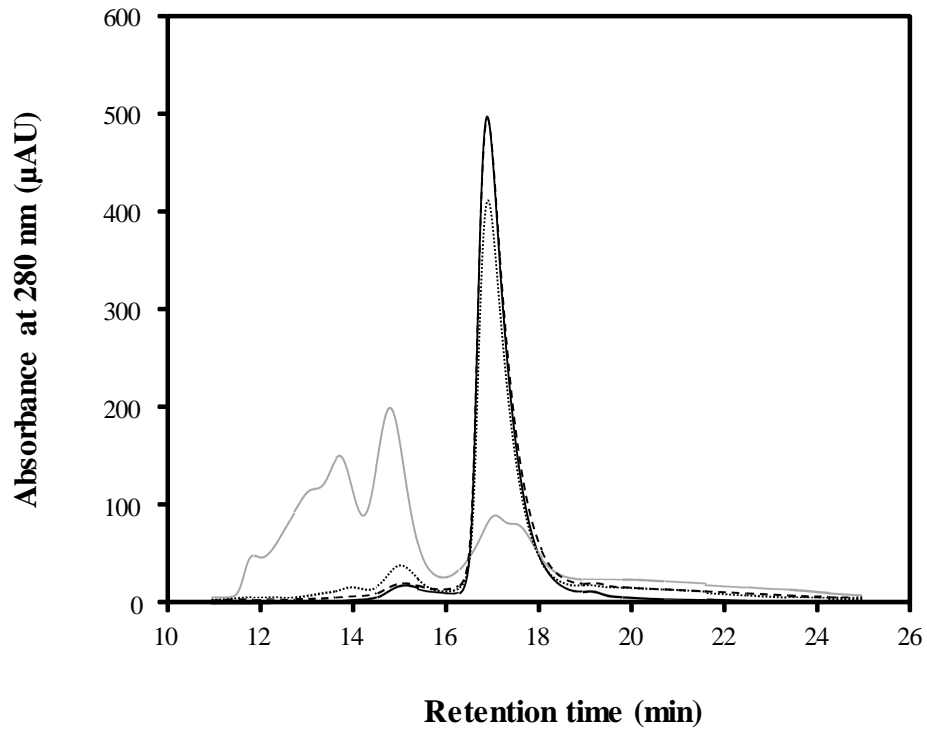
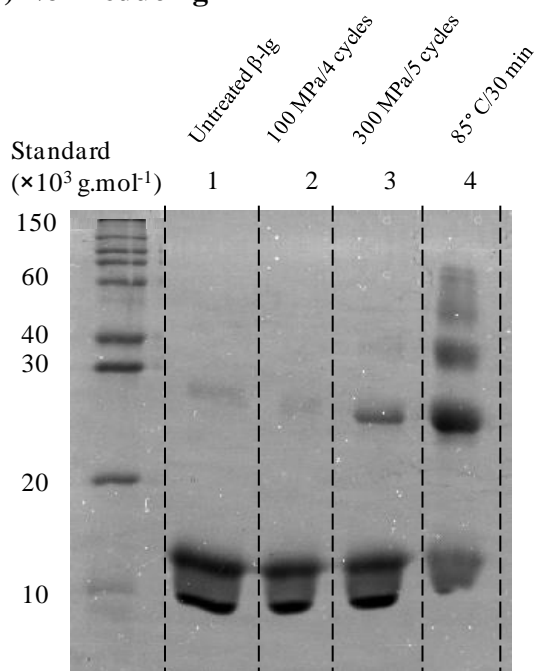


Figure 3.



**Figure 4.**

**(A) Non-reducing**



**(B) Reducing**

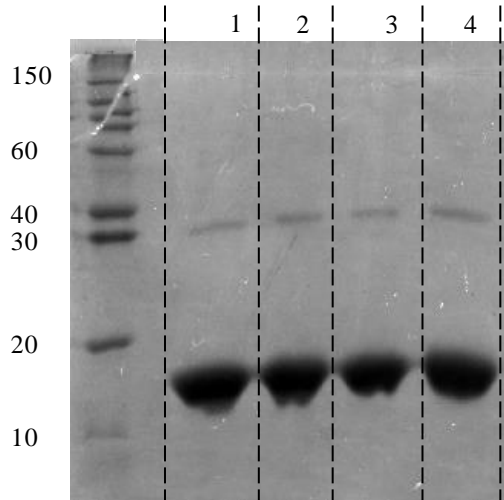


**Figure 5.**

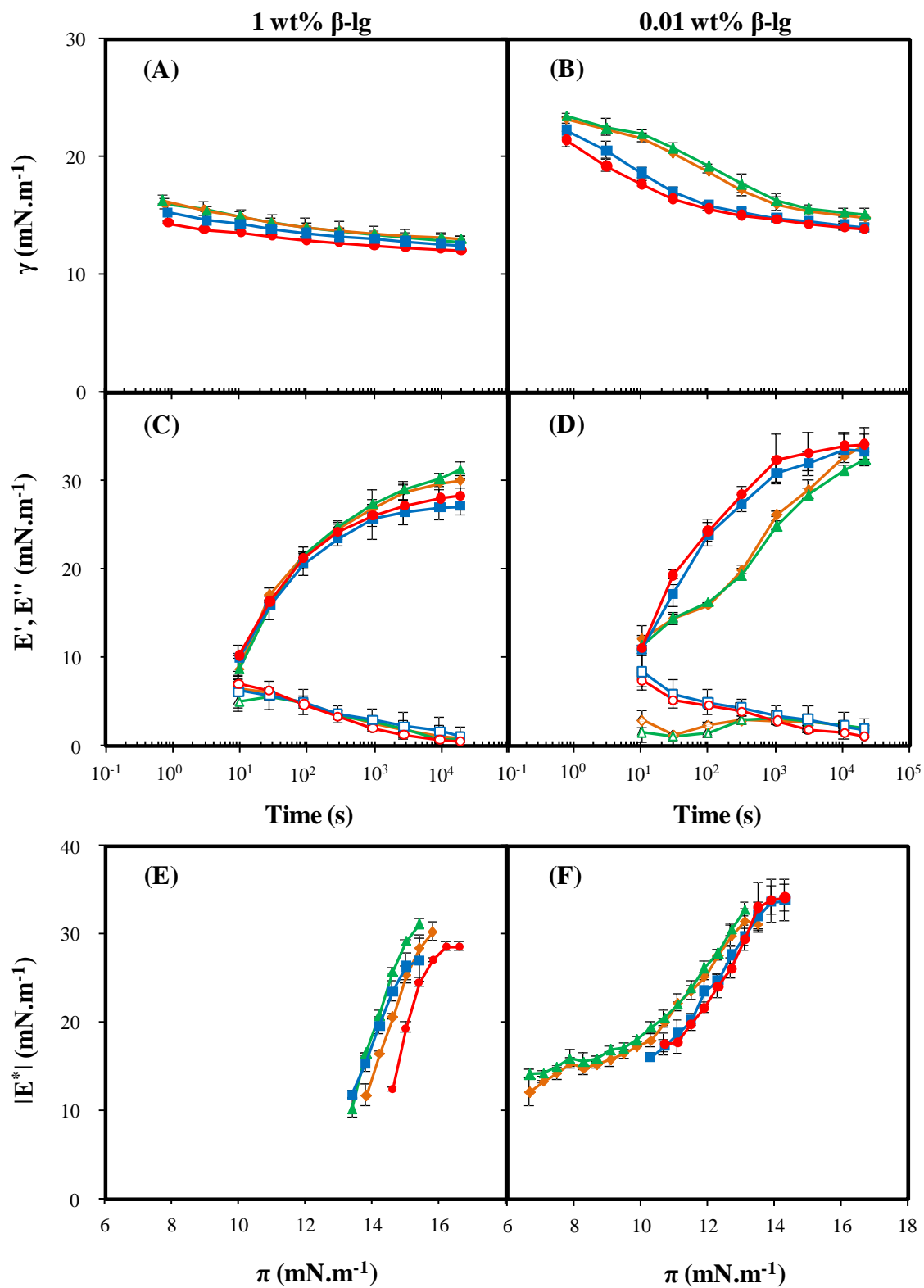
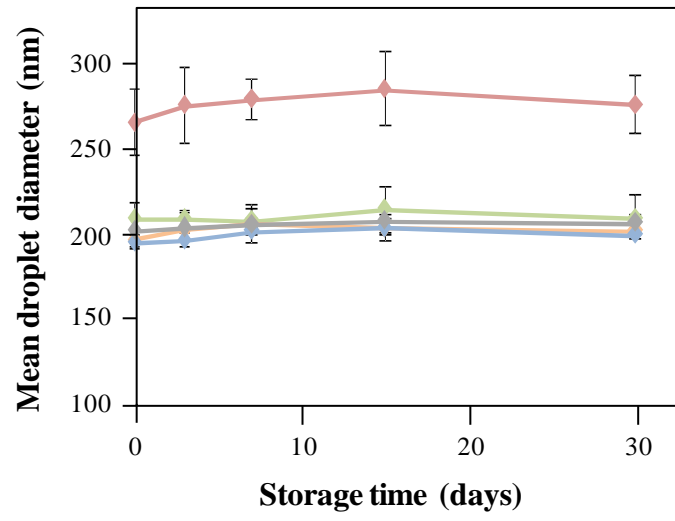


Figure 6.



**Figure 7.**